The Magnesium-Hydrogen System: Transmission Electron Microscopy

T. SCHOBER

The exothermic formation of MgH_2 in Mg has been studied by TEM. The hydrides were formed in the thinned samples by a high pressure technique. Results on the precipitate morphology are reported. The orientation relationship is $(100)_{MgH_2} \parallel (0001)_{Mg}$ and $[001]_{MgH_2} \parallel [\bar{1}\bar{1}20]_{Mg}$. Our results on high purity hydrides confirm previous structural work. Cracking was observed in growing hydrides at the hydride/matrix interface leading to an 'onion structure'. Dehydriding was found to occur also through the formation of internal H_2 bubbles in the MgH_2 precipitates. A model for the $Mg \rightarrow MgH_2$ transformation is presented and the lattice expansion is expressed in terms of the dipole force tensor approach. Finally, the implications of the present results on recent kinetic models by Rudman are discussed.

INTRODUCTION

THE system Mg-H has several important aspects. The exothermically formed hydride MgH_2, which is a tetragonal, ionic compound with an appreciable covalent contribution[1] has been considered as a convenient storage medium for hydrogen for automotive and heat storage applications.[2-7] In this context numerous studies were undertaken concerning reaction kinetics,[8-18] thermodynamics[19] and catalytic surface effects.[20-22] On the other hand, there exist also dilute, endothermic solutions of H in Mg (with H occupying tetrahedral sites) with well defined solubility limits.[23-26]

This work presents a TEM study of the precipitation of the hydride phase MgH_2 in high-purity Mg, its structure and morphology. Emphasis is also placed on the question whether support could be obtained for recent models of the hydriding process in Mg.[14,15]

The structure of MgH_2 is tetragonal, with $a = 0.45025$ nm, $c = 0.30123$ nm.[27] The space group is $P4_2/mnm$. The atomic positions are 2Mg in (000) (1/2 1/2 1/2) and 4H in $\pm$ (xx0) $(1/2 + x, 1/2 - x, 1/2)$ with $x = 0.306 \pm 0.003$,[27] a schematic drawing of MgH_2 is presented in Fig. 1. Further high-pressure phase transitions of MgH_2 were recently reported.[28] In the course of the study it was found that MgH_2 reflections may have to be separated from reflections of the following extraneous phases: $Mg(OH)_2$, hexogonal (trigonal), S.G. $P\bar{3}M1$; MgO, cubic, S.G. FM3M. Magnesium hydroxide may arise here from the reaction of the hygroscopic MgH_2 with water vapor from the air.

EXPERIMENTAL

High purity Mg (99.99 pct) was used in this study. 3 mm discs were punched from annealed 50 μm ribbons and electropolished for TEM using either one of the following solutions A and B. The first one was specially developed for this study.[29]

Solution A	Solution B
20 g LiCl 100 ml glycerine in 1 l CH_3OH 75 V, 220 mA Flow Rate 2.5, -10 °C (Tenupol polishing apparatus)	5 pct $HClO_4$ in CH_3OH 70 V, 200 mA -10 °C, Flow Rate 10 (Tenupol polishing apparatus)

In the work relating to the formation of the MgH_2 phase, hydrogen charging was performed after the final electropolishing step. The reverse procedure (hydriding and subsequent preparation for TEM) would lead to insurmountable difficulties. Also, inspection of the as-polished foils reveals no second phases or gas bubbles. Occasional round features (as on Fig. 2) are artifacts from polishing and not H_2-bubbles. The 3 mm discs were exposed in an all-metal, high pressure reactor to a high-purity (99.999 pct) hydrogen atmosphere at $\sim 5 \cdot 10^6$ Pa and 270 °C for about 16 h. These conditions ensured the formation of large hydride patches in the thinned portions of the Mg samples. Due to the

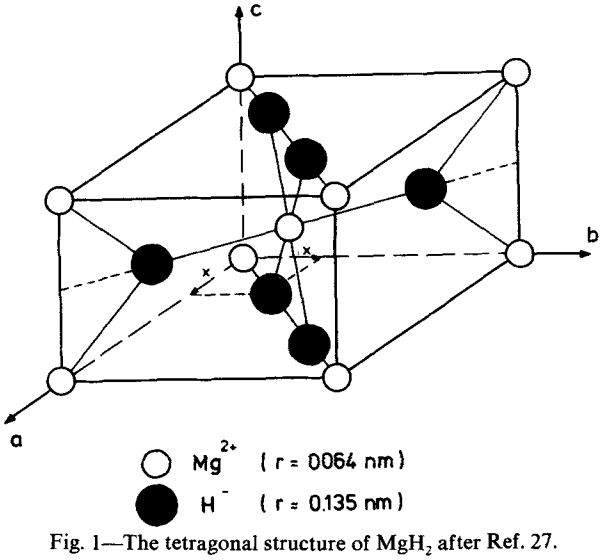

Fig. 1—The tetragonal structure of MgH_2 after Ref. 27.

T. SCHOBER is staff scientist at the Institut für Festkörperforschung, Kernforschungsanlage Jülich, 5170 Jülich, Germany. He is temporarily at Materials Science Division, Bldg. 212, Argonne National Laboratory, Argonne, IL 60439.

Manuscript submitted June 26, 1980.

ISSN 0360-2133/81/0611-0951$00.75/0

instability of the MgH_2 in moist atmosphere, the samples were examined immediately after preparation, or else stored in a desiccator.

Complications also arose from the radiation damage in MgH_2 by the 120 kV electrons. The structure was found to be very sensitive at room temperature and transformed to a fine, polycrystalline structure within seconds of observation time. Also, electron beam heating was believed to play a certain role although a temperature of 290 °C has to be reached to produce an equilibrium pressure of 10^5 Pa[4]. Severe electron radiation damage in ionic and covalent crystals is normal. For a thorough discussion, see for instance, Ref. 30. The problems of radiation damage could be overcome to a large extent by use of the cooling holder of the TEM at a temperature between −130 and −150 °C. At these temperatures, MgH_2 precipitates could be examined for several minutes with only a slight decrease in crystal perfection.

RESULTS

Precipitate Morphology

After hydrogenation large 'blocky' patches (1 to 50 μm in size) of the hydride phase could be observed (fig. 2). These areas were further subdivided by domain or twin boundaries into smaller single-crystal regions, a few μm in diameter, which were well suited for selected area diffraction patterns. In a few cases, there was a high density of thin twins producing extensive streaking in reciprocal space. An analysis of these streaks resulted in a {011}-type twin plane. The observed simple domain pattern was in agreement with the tetragonal crystal structure. The hydride MgH_2 did not precipitate in the form of thin plates on a well defined habit plane. The close proximity of the foil surfaces is not found to have much effect on the morphology of hydride precipitation. Even in the very thick areas (~1 μm) the 'blocky' morphology was observed rather than thin plates. Also, SEM micrographs of hydride precipitation in bulk samples display the 'blocky' hydrides. We believe, therefore, that the morphology (and also the crystallography) observed in the TEM work is representative of the bulk. The patches had rather planar Mg-MgH_2 interfaces which were shown by trace analysis to be parallel to low-index planes of the MgH_2 structure such as {011}, {001}, {110} and {lll}.

The orientation relationship between MgH_2 and Mg was obtained from several SAD patterns showing both phases (Fig. 3) by transferring this information onto stereographic projections. It was found that $(100)_{MgH_2} \parallel (0001)_{Mg}$; and $[001]_{MgH_2} \parallel [\bar{1}\bar{1}20]_{Mg}$. MgH_2-regions displayed, in general, a somewhat higher dislocation density than the parent phase. (This increase may not

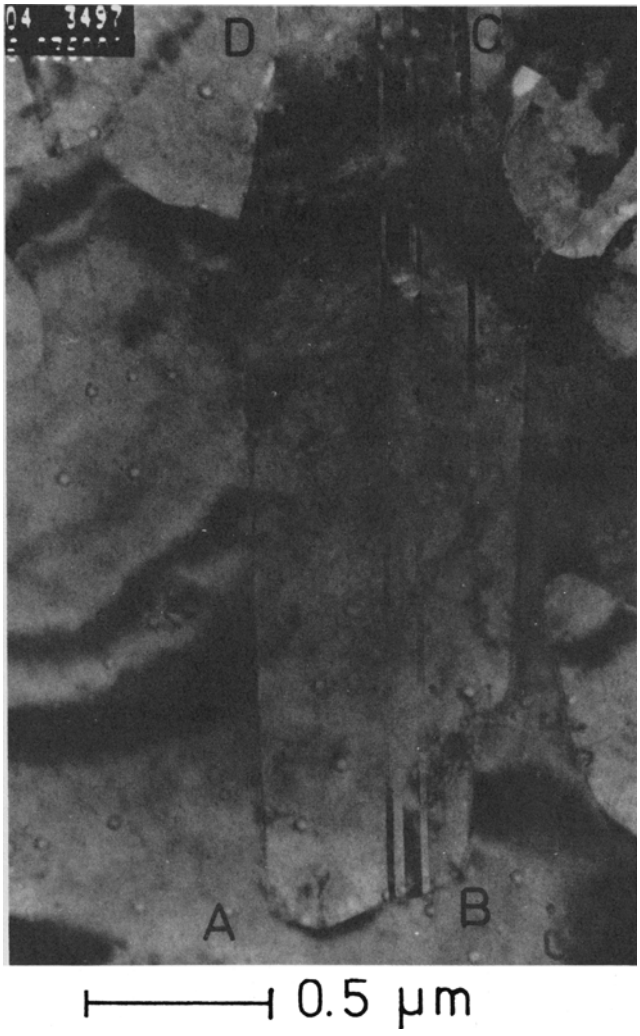

Fig. 2—MgH_2-precipitate in Mg inside points A, B, C, D. Note internal twin boundaries which are of {011} type. BF, 120 kV, kinematical.

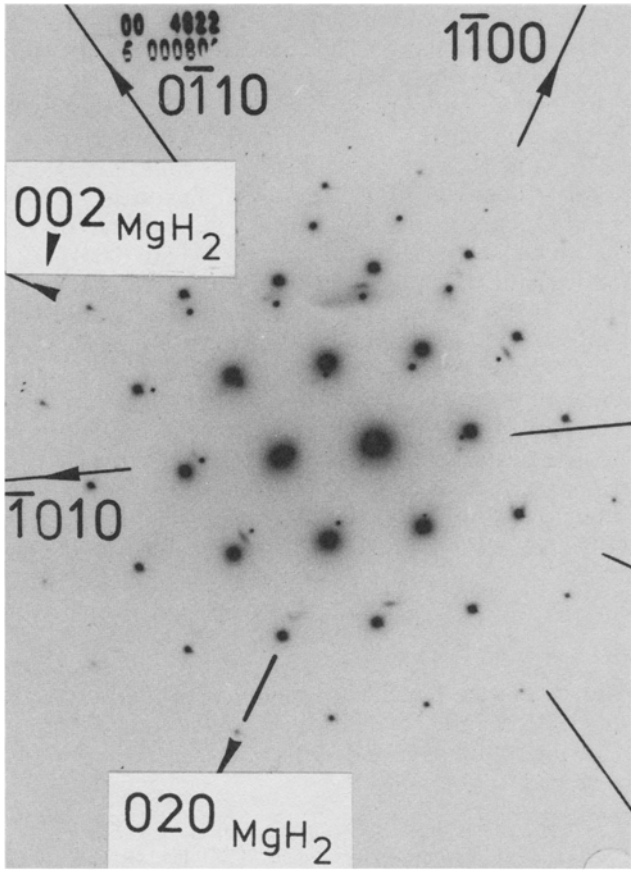

Fig. 3—A typical SAD pattern showing reflections of both phases, Mg and MgH_2. The particle contained no twin boundaries. The sharp reflections on a regular hexagonal grid pertain to Mg.

be visible on all micrographs due to the poor contrast of dislocations in Mg.) This is also indicated by a broadening of MgH_2 reflections. This increased dislocation density was certainly produced by the migrating phase boundary. It is emphasized that at least the smaller precipitates did not show internal or peripheral cracks and were solidly embedded in the matrix.

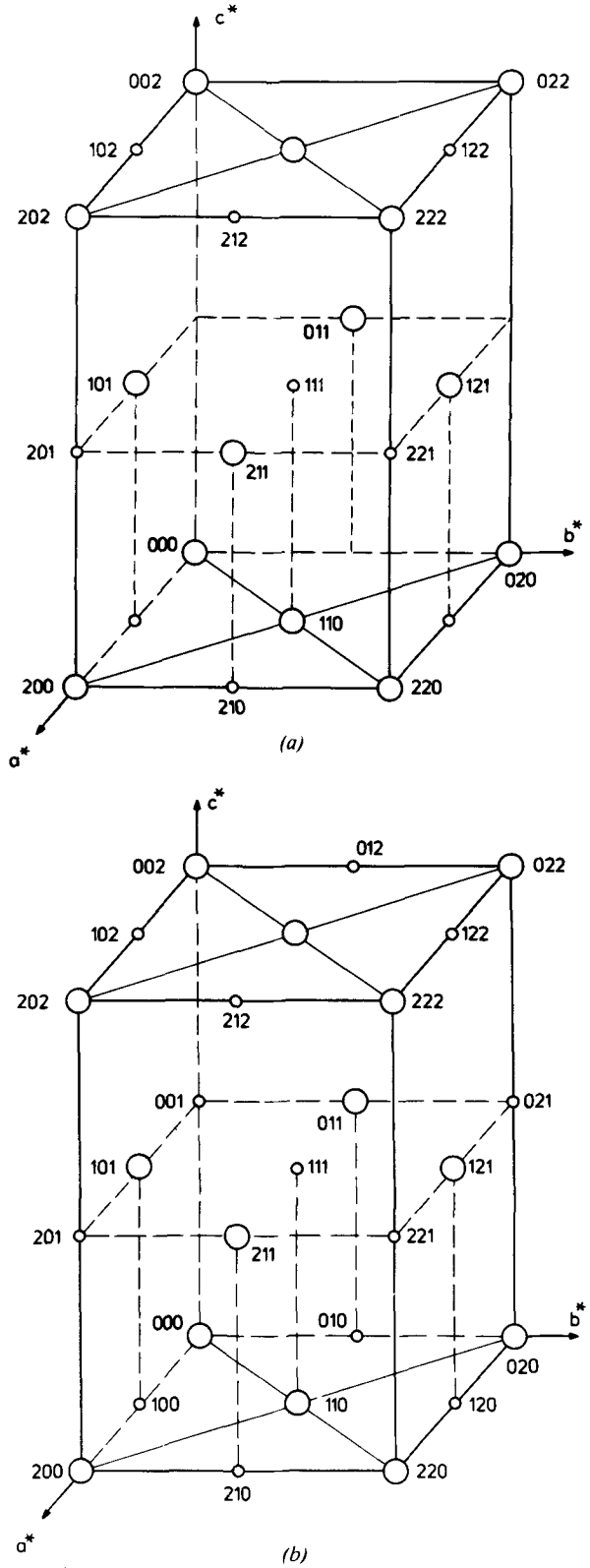

Fig. 4—The reciprocal lattice of the MgH_2 structure. Large circles corresponding to metal lattice reflections, small circles: hydrogen superlattice(*a*) containing extinction conditions for this structure[31] (*b*) additional reflections may appear due to double diffraction. Sections of this reciprocal lattice are actually observed by TEM.

Structure

The reciprocal lattice for the MgH_2 structure as obtained from Ref. 31 is graphically shown in Fig. 4(*a*). Certain hydrogen superlattice reflections are missing. Also, metal lattice reflections occur only when $(h + k + l) = 2n$. In practice, however, the reciprocal lattice to be observed due to double diffraction is shown in Fig. 4(*b*). Here, all reflections shown may occur. Our observed SAD patterns correspond precisely to sections of Fig. 4(*b*) as Fig. 5 demonstrates. The low intensity spots (where $(h + k + l)$ is odd) in Fig. 5 are hydrogen superstructure reflections. These would be invisible in X-ray studies. We may therefore conclude that our results are a direct confirmation of the earlier conclusions.[27] We may point out, however, that the early work[27] was done on powder (with only (87.8 pct MgD_2) of an isotopic compositon of about $D_{0.9}H_{0.1}$ (The gas phase had a 9.6 at .pct H_2 contamination in the deuterium gas) while this study was performed with single crystal areas with 100 pct MgH_2 and 100 pct H.

Precision SAD's containing sharp Mg reflections as internal calibration yielded the following lattice parameters for MgH_2: $a = 0.450 \pm 0.001$ nm; $c = 0.303 \pm 0.001$ nm. The present value of a is, within experimental limits, the same as in the neutron study;[27] whereas c is slightly larger. We also note that no phase transition was observed in MgH_2 down to -150 °C.

Growth of Hydrides

In our thinned samples the following sequence of events was observed with increasing hydriding time: 1) small faceted hydride particles are formed at many spots: they extend through the foil. 2) At a critical size (~5 to 10 μm) partial cracking occurs around the periphery of the MgH_2 particles and the hydride front has a new plane of attack. By repeated cracking at the periphery an 'onion structure' of hydrided layers is formed. A typical example is shown in Fig. 6 (details in Figure Caption). Finally, the large hydride patches impinge and form larger agglomerates. The initial stages of hydriding of bulk samples as observed by SEM and optical microscopy were quite similar: first, small, white, faceted particles appeared on the surface. In later stages, these nuclei grew larger and coalesced. Finally, a whitish hydride layer covered the samples.

Recrystallization and Decomposition

The large single crystal regions of MgH_2 were found to be unstable at higher temperatures (>300 °C) and/or slightly oxidizing atmospheres. They transformed to a fine grain structure. As an example Fig. 7 shows the same area as in Fig. 2 after exposure to the combined effects of electron irradiation and beam heating. Many small grains have apparently formed; typical sizes are 10 to 20 nm. The SAD patterns reveal

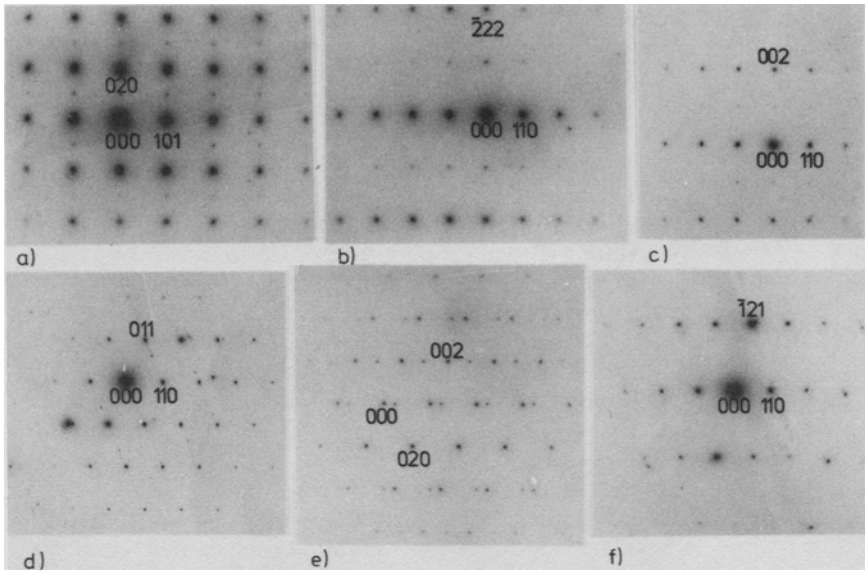

Fig. 5—(*a*) to (*f*): SAD patterns from MgH_2 single crystal areas corresponding to the reciprocal lattice in Fig. 4(*b*). Fig. 5(*e*) contains also weaker reflections from a twin lamella.

the presence of rings corresponding to a complex mixture of Mg, MgH_2 and MgO reflections.

Furthermore, deliberate dehydriding runs in the heating stage of the TEM showed the simultaneous appearance of hydrogen bubbles and the formation of the fine grain structure. A typical case is presented in Fig. 8 (Details in Figure Caption). The final dehydriding state of previously hydrided areas was a loose structure of Mg grains with sizes below 100 to 200 nm. Thus, areas within the Mg matrix which are hydrided may not be converted again to the initial matrix orientation by dehydriding. Here lies a fundamental difference in the hydriding- dehydriding behavior between Mg and metals like Nb, Ti, Ta and V. (Hydrided patches in Nb, for instance, return to the same matrix orientation after dehydriding. Only the dislocation density in the affected area is increased considerably.[32]) Finally, we note that dehydriding is accompanied by a plastic deformation of the surrounding matrix as witnessed by the emission of dislocation loops. This plastic deformation may not be visible on all micrographs of similarly treated samples depending on the grain orientation. Figure 9 shows an example of a MgH_2 particle in the initial stages of dehydriding.

Fig. 6—Larger MgH_2 area in Mg showing the onion skin structure arising from repeated cracking around the periphery of the growing MgH_2 particle. BF, 120 kV, kinematical.

DISCUSSION

The interesting orientation relationship between Mg and MgH_2 may be visualized in Fig. 10. Note that only the metal atoms are shown in Fig. 10. There is one plane common to both crystals (containing the vectors **a** and **c**) where there is only a 6 pct length change along $\mathbf{a}_3$ and 13.6 pct along [0001]. Here, the crystals match rather well and this 'invariant' plane does not rotate during the transformation. Figure 10 shows a proposed model of the transformation: the metal atoms have to move only fractions of atomic distances along the dotted lines to reach their positions in the MgH_2-structure.* The above orientation relationship was obtained from untwinned precipitates. Twinning could provide a means of accommodating the mismatch, but it does not seem to be the main mechanism or to be required here. Quite often large MgH_2 particles could be observed without any twin boundaries at all.

*The orientation relationship reported here is different from any of those reported by Bradbrook *et al* (*J. Nucl. Mat.* 1972, vol. 42, p. 142) for zirconium hydride in hcp Zr. This is not unexpected, however, because the fcc structure of the metal sublattice in zirconium hydride is much different from that of MgH_2.

From Fig. 10 we can also obtain information on the hydrogen-induced lattice expansion by considering equivalent volumes of unit cells in Mg and MgH_2. When we take a Mg hcp unit cell as reference we obtain the volume expansion shown in Fig. 11. For purposes of comparison we have included data on the FeTi-H system. It is seen that the slopes are rather similar. To a first approximation we may obtain information on the lattice expansion (as a function of hydrogen content) at low concentrations by considering the expansion of the concentrated phases and assuming a linear behavior. (This approach works surprisingly well for Nb[32] and FeTi[33]). For low concentrations and isotropic expansion we may apply the standard dipole force tensor approach as recently reviewed by Peisl.[34] This approach is not affected by possible 'thin film' effects since the lattice parameters used are virtually identical with the'bulk' parameters.

The volume change $\Delta V/V$ upon hydriding is

$$\frac{\Delta V}{V} = c \cdot \frac{\Delta v}{\Omega} \qquad [1]$$

(c = concentration, Δv = characteristic volume change per H atom, Ω = mean atomic volume of a metal atom). This volume change is given for a random distribution and a cubic crystal by:

$$\frac{\Delta V}{V} = \frac{c}{3\Omega} \cdot K \cdot TrP_{ij} \qquad [2]$$

(K = compressibility, P_{ij} the dipole force tensor). From Fig. 11 and Eq. [1] we obtain for Mg-MgH_2:

$$\frac{\Delta v}{\Omega} = 0.15731$$

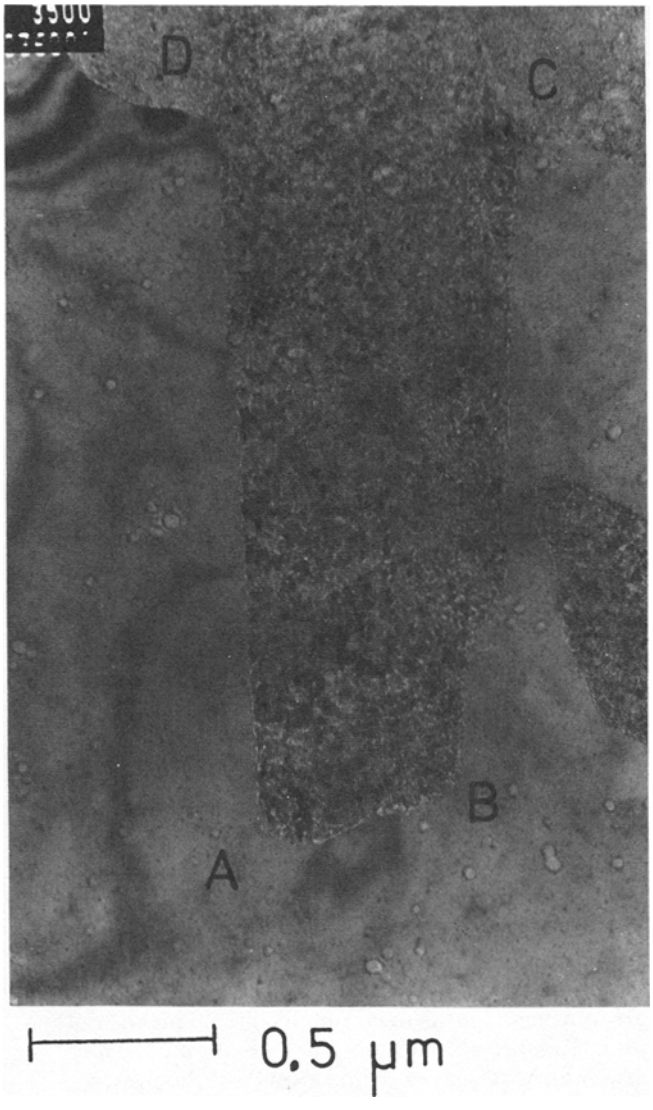

Fig. 7—Same area as in Fig. 2 (inside points ABCD) after electron beam heating in the TEM. The originally single crystal areas have transformed to a fine grain structure containing small grains of Mg, MgH_2 and MgO. Many small hydrogen bubbles have formed internally and at the MgH_2-Mg interface. ABCD denotes again the shape of the original hydride plate. BF, 120 kV, kinematical.

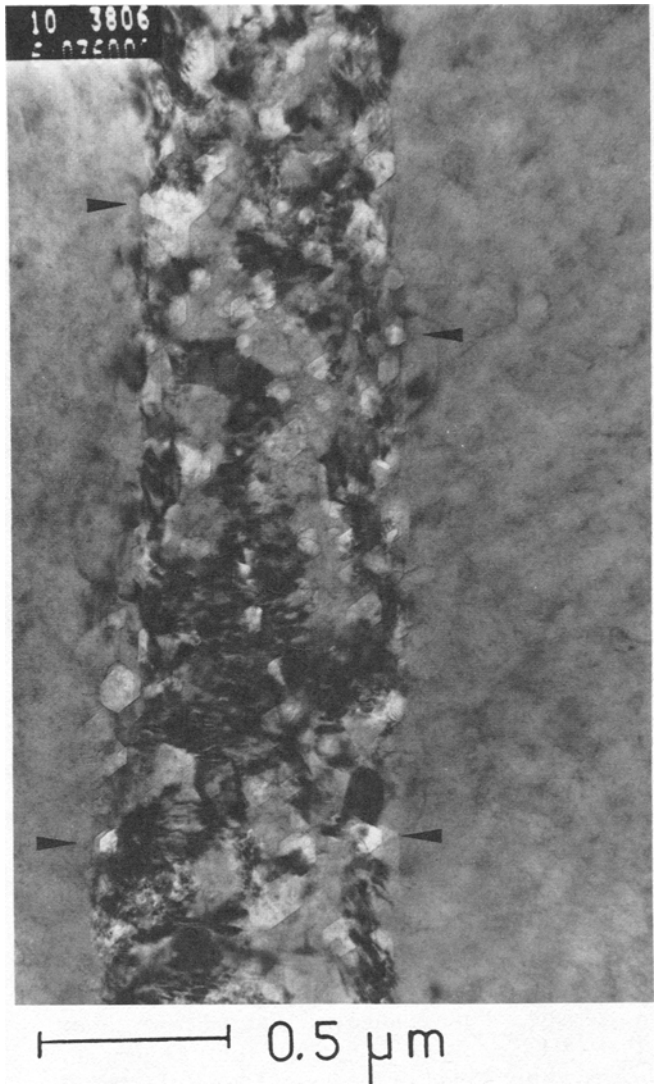

Fig. 8—Dehydrided area in Mg. The vertical ribbon was originally a MgH_2 precipitate. The sample was heated shortly to 250 °C in the TEM in the absence of electron illumination. Small grains of Mg (and some MgO) and a high density of H_2—bubbles may now be observed. Arrows denote some of the larger bubbles. Tilting allows differentiation between Mg-grains and gas bubbles. During the heating the microscope vacuum was observed to deteriorate dramatically. H_2 is the only gas that could be evolved from the sample at such a rate. The Mg grains have lost their relationship to the matrix, BF, 120 kV, kinematical.

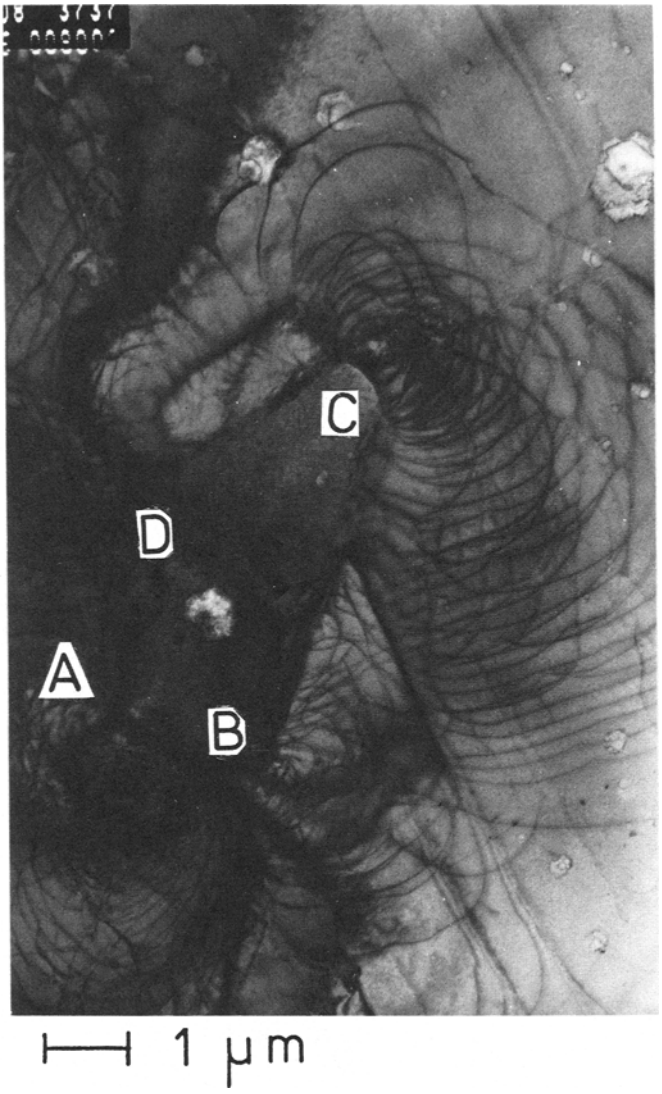

Fig. 9—MgH_2 particle (marked A, B, C, D) in Mg after warming to ~150 °C in the TEM without electron illumination. Dehydriding has started as witnessed by the emission of dislocations from the particle. These dislocation loops were shown to be emitted by small H_2 gas bubbles in the interface. BF, 120 kV kinematical.

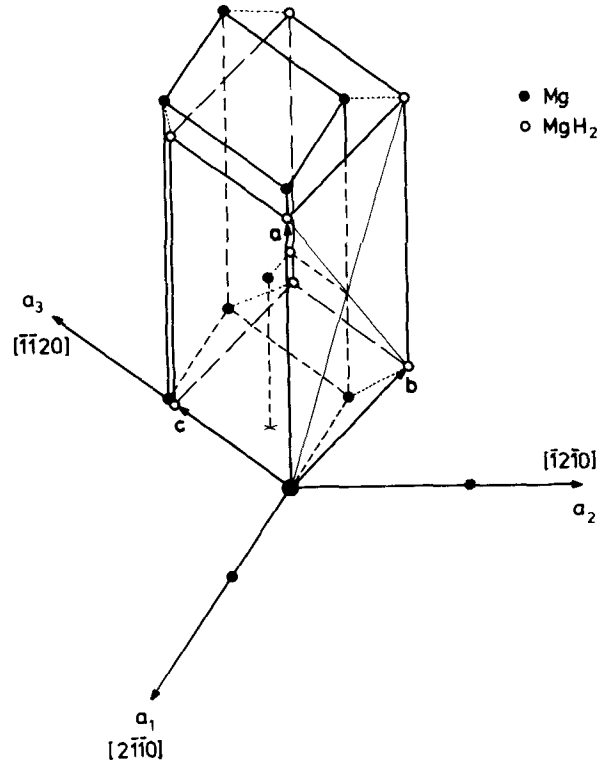

Fig. 10—Graphical presentation of the orientation relationship between two unit cells of Mg and one unit cell of MgH_2 (Only the metal atoms are shown). Note good match in the plane containing vectors **a** and **c**. For the Mg → MgH_2 transformation the atoms have only to move along the dotted lines to their new positions.

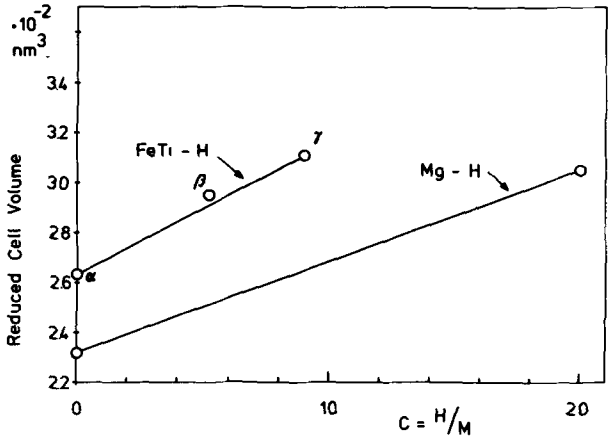

Fig. 11—Lattice expansion during the formation of MgH_2 as based on the model in Fig. 10. For purposes of comparison the values for the FeTi-H system are included.

For other M-H hydrogen systems the following values of $\Delta\nu/\Omega$ were obtained: 0.174 (Nb),[34] 0.155 (Ta),[34] 0.19 (V),[34] 0.19 (Pd),[34] 0.199 (FeTi).[33] Using the Mg compression modulus $1/K = 0.3736 \cdot 10^{11}$ Pa we obtain for the trace of the dipole force tensor: $TrP_{ij} = 2.556$ eV (Mg-H system), which is (due to the smaller compression modulus) considerably lower than values listed for other systems: 10.1 eV (Nb),[34] 9.0 eV (Ta),[34] 7.03 eV (V)[34] and 9.3 eV (FeTi).[33] For the characteristic volume change per H atom $\Delta\nu$ we obtain for the MgH system: $\Delta\nu = 3.65 \cdot 10^{-3}$ (nm)³. This quantity $\Delta\nu$ is within 25 pct of the value $2.9 \cdot 10^{-3}$ (nm)³ found to be valid for many other materials.[34]

As to the reaction kinetics, Rudman[14,15,19] has suggested that 1) the hydriding kinetics are determined by H-diffusion through the growing hydride layer, 2) the dehydriding kinetics are governed by the rate of H-diffusion through the growing metal, and 3) the diffusing species is the H-anion.[35] Although we concur qualitatively with these conclusions, the present experiments suggest the following remarks and criticism of the above model: 1) the initial step of hydriding is the nucleation, growth and coalescence of 3-dimensional MgH_2 clusters (This is in complete agreement with other work in Refs. 10–12) and not the formation of a thin continuous MgH_2 layer, 2) the growth of the present MgH_2 precipitates should be at least partially controlled by H-diffusion along the Mg-MgH_2 interface. (This interface was observed here to be a regular dislocation phase boundary. Presumably, it short-circuits H-diffusion through the bulk and offers convenient points of

entry into the lattice). Thus a phase boundary diffusion term should be incorporated in Rudman's model. 3) It is also shown here, that flaking or cracking along the Mg-MgH_2 interface is an important phenomenon. It creates repeatedly fresh surface area and reduces thereby the diffusion distances. 4) as seen in Fig. 9, dehydriding may also occur by the formation of H_2-bubbles in the hydride and at the Mg-MgH_2 interface. Thus, an additional internal sink term should be added to the dehydriding model.

Adding to the considerable complexity of hydriding/dehydriding kinetics are also the following factors: 1) Sublimation of Mg, formation of MgH_2 in the gas phase; 2) condensation of Mg particles and subsequent hydrogenation; 3) the instability of single-crystal hydride precipitates at elevated temperatures and/or oxidizing atmosphere(see for this point also Ref. 36) and the formation of very fine Mg grains in the dehydriding cycles.

ACKNOWLEDGEMENT

Helpful discussions with Prof. H. Wenzl and Dr. D. G. Westlake are acknowledged. The technical assistance by M. Jansen is also appreciated.

REFERENCES

1. C. M. Stander and R. A. Pacey: *J. Phys. Chem. Solids*, 1978, vol. 39, p. 829.
2. D. L. Douglass: *Met. Trans. A*, 1975, vol. 6A, p. 2179.
3. J. J. Reilly and R. H. Wiswall: *Inorg. Chem.*, 1967, vol. 6, p. 2220.
4. J. J. Reilly: *Hydrogen: Its Technology and Implications*, vol. 2, p. 13, CRC Press, Inc. Cleveland, Ohio, 1978.
5. J. J. Reilly and G. D. Sandrock: *Sci. Am.*, 1980, vol. 242, p. 118.
6. H. Buchner: *Proc. 2nd World Hydrogen Conf., Zürich Switzerland, 1978*, vol. 4, p. 1749, Pergamon Press, New York.
7. W. Rummel: *Siemens Forsch. Entwicklungsber*, 1978, vol. 7, p. 44.
8. J. Renner and H. J. Grabke: *Z. Metallkd.*, 1972, vol. 63, p. 289.
9. B. Tanguy and J. L. Soubeyroux, M. Pezat, J. Portier, P. Hagenmuller: *Mater. Res. Bull.*, 1976, vol. 11, p. 1441.
10. C. M. Stander: *Proc. Electron Microscopy Soc. of Southern Africa (Johannesburg)*, 1976, vol. 6, p. 77.
11. C. M. Stander: *J. Inorg. Nucl. Chem.*, 1977, vol. 39, p. 221.
12. C. M. Stander: *Z. Phys. Chem., NF*, 1977, vol. 104, p. 229.
13. M. H. Mintz, Z. Gavra and Z. Hadari: *J. Inorg. Nucl. Chem.*, 1978, vol. 40, p. 765.
14. P. S. Rudman: *J. Appl. Phys.*, 1979, vol. 50, p. 7195.
15. A. Karty, J. Grunzweig-Genossar and P. S. Rudman: *J. Appl. Phys.*, 1979, vol. 50, p. 7200.
16. B. Vigeholm, J. Kjøller and B. Larsen: *Proc. Int. Symp. Prop. and Appl. of Metal Hydrides, Colorado Springs, Col. 1980, J. Less-Comm. Met.*, 1980, vol. 74, p. 341.
17. M. H. Mintz, J. Gavra, G. Kimmel and Z. Hadari: *Proc. Int. Symp. Prop. and Appl. of Metal Hydrides, Colorado Springs, Col. 1980, J. Less-Comm. Met.*, 1980, vol. 74, p. 263.
18. M. Pezat, B. Darriet and P. Hagenmuller: *Proc. Int. Symp. Prop. and Appl. of Metal Hydrides, Colorado Springs, Col. 1980, J. Less-Comm. Met.*, 1980, vol. 74, p. 427.
19. P. S. Rudman: *Int. J. Hydrogen En.*, 1978, vol. 3, p. 431.
20. Th. von Waldkirch, A. Seiler, P. Zürcher and H. J. Matheiu: *Mater. Res. Bull.*, 1980, vol. 15, p. 353.
21. L. Schlapbach and D. Shaltiel: *Mater. Res. Bull.*. 1979, vol. 14, p. 1235.
22. J. Genossar and P. S. Rudman: *Z. Phys. Chem., NF*, 1979, vol. 116, p. 779.
23. J. S. Lally and P. G. Partridge: *Philos. Mag.*, 1966, vol. 13, p. 9.
24. P. Tzanétakis, J. Hillairet and V. Lévy: *Scr. Metall.*, 1976, vol. 10, p. 1131.
25. R. Fromageau, C. Mairy and P. Tzanétakis: *Scr. Metall.*, 1980, vol. 14, pp. 395–398.
26. A. C. Chami, J. P. Bugeat and E. Ligeon: *Radiat. Eff.*, 1978, vol. 37, p. 73.
27. W. H. Zachariasen, C. E. Holley and J. F. Stamper: *Acta Crystallogr.*, 1963, vol. 16, p. 352.
28. J.-P, Bastide, B. Bonnetot, J.-M. Létoffé and P. Claudy: *Mater. Res. Bull.*, 1980, vol. 15, p. 1215.
29. T. Schober and M. Jansen: *Prakt. Metallogr.*. 1980, vol. 17, p. 511.
30. J. R. Fryer: *The Chemical Applications of Transmission Electron Microscopy*. Academic Press, London 1979.
31. *International Tables for X-ray Crystallography*, vol. I, the Kynoch Press, England, 1976.
32. T. Schober and H. Wenzl: *Hydrogen in Metals II*, G. Alefeld, J. Völkl, eds. *Topics in Applied Physics*, vol. 29, p. 11, Springer Verlag, Berlin, 1978.
33. T. Schober and W. Schäfer: *Proc. Int. Symp. Properties and Application of Metal Hydrides, Colorado Springs, 1980, J. Less-Comm. Met.*, 1980, vol. 74, p. 23.
34. H. Peisl: *Hydrogen in Metals I*, vol. 28, *Topics in Applied Physics*, G. Alefeld and J. Völkl, eds., Springer Berlin, 1978.
35. Z. Luz, J. Genossar and P. S. Rudman: *Scr. Metall.*, 1980, vol. 14, p. 275.
36. G. Bertrand, M. Comperat, M. Lallemant and G. Wattelle: *J. Solid State Chem.*, 1980, vol. 32, p. 57.